



INFLUENCE OF WELDING VARIABLES ON THE MICROSTRUCTURAL AND TENSILE PROPERTIES OF 304L AUSTENITIC STAINLESS STEEL HEAT AFFECTED ZONE

Oyetunji, A

Department of Metallurgical and Materials Engineering, The Federal University of Technology, Akure, Ondo State, Nigeria

Corresponding author: akinlabioyetunji@yahoo.com

Received 18 June, 2014; Revised 29 May, 2015

ABSTRACT

This work investigates the effects of welding speeds and power inputs at different ranges on the Heat Affected Zone (HAZ), microstructural characteristics and tensile behaviour of type 304L austenitic stainless steel. Chemical analysis of the as-received 304L austenitic stainless steel was done to determine its chemical composition. Thereafter, the as-received 304L austenitic stainless steel plate was cut with hacksaw into sample of dimensions 70 mm length, 45 mm breadth and 8 mm thickness, thirty samples were produced in all with ten samples each assigned to group A, B and C respectively. The grouped samples were further cut into two equal halves with hacksaw and welded using Gas Metal Arc Welding (GTAW) process and 304L electrode to produce butt joint HAZ square geometry samples. The obtained HAZ samples and as-received sample were machined to standard tensile test specimens, and tensile test was made using standard approaches. The HAZ and as received specimens were prepared for microscopy studies, and etched in a solution of 1 ml HCl + 3 ml HNO₃ + 1 ml glycerol, and the microstructures were examined using metallurgical microscope at a magnification of 400xx. Results obtained show that the microstructures are composed mainly of mixture of austenite and ferrite phases, also variations in volume fraction and grain size of the phases were observed at the different welding speeds and power inputs. In addition, chromium carbide formation and precipitation due to sensitization was seen at the grain boundaries. Also, optimum ultimate tensile strength (UTS) and yield strength (YS) were obtained for HAZ sample at moderate (4.5 mm/s) welding speed, and optimum % elongation at slow welding speed. Optimum UTS and YS were obtained for HAZ sample at power input of 9.2 KW, and optimum % elongation at 12.00 KW. Generally, when compared with the as-received sample, remarkable influence of the welding variables on tensile characteristics of the material's HAZ was noticed.

Keywords: 304L austenitic stainless steel; tensile behavior; microstructures; welding variables.

INTRODUCTION

The type 304L Austenitic Stainless Steel (ASS) is a versatile material whose engineering properties have been well acknowledged in various applications requiring welding. It is the most weldable of all the 304 series [1], and this has underscored its successful use as structural steel parts in chemical, mechanical, automobile, metallurgical and nuclear, and cryogenic applications such as the handling of Liquefied Natural Gases (LNG) [2]. However, failures of this material at the welded parts have been recorded in service under static and dynamic loading conditions [1, 2]. Generally, metallurgical approaches including alloying and heat treatments [3] have been



used to enhance the service integrity of steel materials, but during welding, the microstructure of the welded area are altered in the regions of the HAZ which attain temperatures of over 1000°C [4]. Hence neither alloying nor heat treatment prior welding has provided the needed recipe to welded joints failures.

Welding as a local melting-freezing process is known to create high temperature gradients in the metal around the weld [2, 4]. Research findings have revealed that the performance of the welded structure is usually limited by cracks initiation within the Heat-Affected Zone (HAZ) of the base material, particularly within the coarse- grain region of the HAZ adjacent to the weld metal [5]. Hence, the role of heat affected zones at enhancing weld joint integrity cannot be overemphasized. During welding, the weld thermal cycle produces differently featured heat-affected zone (HAZ) microstructures which correspond to different mechanical properties [3, 6], and if the microstructural changes in the HAZ are not controlled as a result of improper selection of welding variables, the resulting metallurgical structures may be undesirable, and as a consequence, poor weld joint quality may be produced [4]. Choosing suitable welding variables that will produce balanced (optimum or acceptable) HAZ microstructure [7] is one profound means by which materials' weld joint integrity can be ensured [6]. Therefore, adequate fundamental understanding of the behaviour of 304L austenitic stainless steel under varied welding variables is necessary if incidences of weld joints failures are to be mitigated. Consequently, effort was made in this work to investigate tensile characteristics of this material at different ranges of welding speeds and power inputs.

MATERIALS AND METHODS

The material used for this research work is type 304L austenitic stainless steel plate sheet of thickness 8 mm. The sample was obtained from universal steel at Ilupeju, Lagos Nigeria. The chemical composition of the as received 304L austenitic stainless steel plate was done by optical emission spectrometry using AR 4 30 metal analyzer and the result is shown in Table 1.

Table 1: Chemical Composition of the As-Received 304L Austenitic Stainless Steel Plate Sheet

Element	C	Si	S	P	Mn	Ni	Cr	Mo	V	Cu	Nb	Co	Al	Pb	Ca	Zn	Fe
% Wt	0.038	0.649	0.05	0.051	1.859	8.079	18.403	0.319	0.075	0.871	0.104	0.172	0.027	0.013	0.005	0.031	69.65

Sample Preparation

The as- received 304L austenitic stainless steel SS plate was cut with hacksaw into samples of dimensions 70 mm length, 45 mm breadth and 8 mm thickness. A total of thirty samples were produced, they were grouped into A and B, and fifteen samples were contained in each groups.

Welding

Samples with length 50 mm were marked out into square geometry, and cut with hacksaw. Thereafter, one half of the samples were joined to the corresponding ones by Gas Metal Arc Welding (GMAW) process using 304L electrode to produce the square geometry butt joint HAZ samples at a range of welding speeds and power inputs [8,9]. Welding machine with specifications:



GMAW 500; duty 60% and 24.7 KVA input capacity was used. Details of the welding parameters used are presented in Table 2.

Table 2: Welding Parameters for the Square Geometry Butt Joint HAZ Samples

S/N	Varied Parameters Considered and their Ranges	Constant Parameters
1	Welding Speed; Range: Fast (9.5mm/s) Moderate (4.5mm/s) Slow (2.5mm/s)	Square Geometry, GMAW process, 308L electrode, and 9.20KW power input.
2	Power Input (KW); Range: 4.60 9.20 12.00	Square Geometry, GMAW process, 308L electrode, and Moderate speed.

Machining

The obtained butt joint samples as well as the as-received sample were machined to shapes with lathe machine to produce tensile specimens. Machining of the as-received sample was done longitudinally, while that of the welded samples was done across the HAZ of the weldments [9]. The (HAZ and as-received) samples were machined to square shape with diameters of 20 mm at the shoulder and 5 mm at the reduced section respectively to produce the tensile specimens (Fig.1).

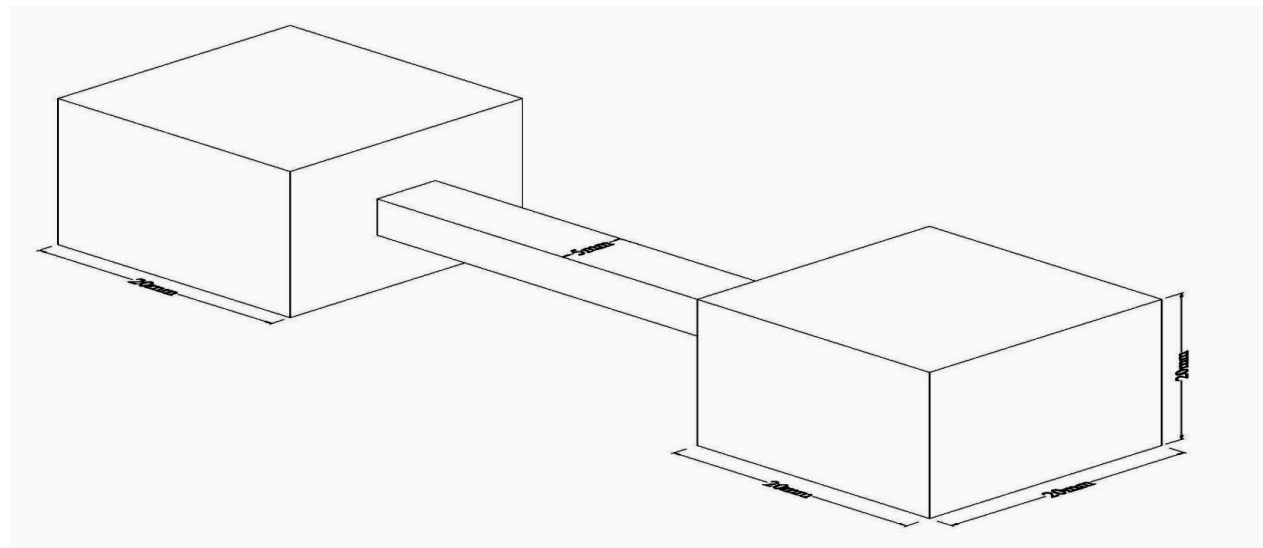


Fig. 1: Tensile Specimen of the Experimental Steel



Tensile Strength

Tensile tests were carried out on the specimens using Instron Universal Testing Machine Model 3369 at the speed of 0.02 mms^{-1} [10]. Appropriate forces and extension were produced and these were converted to stress and strain graph (scaled version of force - extension graph). Thereafter, plots of stress on the vertical axis and strain on the horizontal axis were made [7].

Metallography

Specimens for microscopy studies were prepared from the as-received and HAZ samples by machining to dimensions of 10 mm length, 10 mm breadth and 8 mm thickness, they were mounted on thermosetting material known as Bakelite in order to make them convenient for handling. Thereafter, the surfaces of the specimens were then flattened by filing and grinding using laboratory grinding and polishing machines with a set of emery papers of 240, 320, 400, 600, 1000 and 1200 microns. The grinding was done in order of coarseness of the papers. As each specimen was change from one emery papers to the other, it was turned through an angle of 90° to remove the scratches sustained from the previous grinding. After grinding, the specimens were polished using rotary polishing machine, to give it mirror like surface, a polishing cloth was used to polish the surface of the specimens [9]. The microstructures of the as-received sample and HAZ samples at a range of welding speed and power input were examined after etching in a solution of 1 ml HCl + 3 ml HNO_3 + 1 ml glycerol using metallurgical microscope Model- Axio with camera attached at magnification of 400xx.

RESULTS AND DISCUSSIONS

Microstructure

Results for the as-received and HAZ samples at varied welding speed and heat input are depicted in Figs. 2, 3(a-c) and 4(a-c) respectively. Generally, the phases are composed majorly of austenite and ferrite. Also, chromium carbide formation and precipitation due to sensitization was observed at the grain boundaries. After etching, the ferrite phase was obtained as a lighter phase in between the darker austenite phase [12], and only a little difference was observed to exist between microstructure of the as-received sample and that of the HAZ samples at varied range of welding speeds and power inputs. The ferrite phase is seen to be relatively more dispersed in the austenite matrix of the as-received sample (Fig.2) as compared to austenite matrix of the HAZ samples in Figs. 3(a-c) and 4(a-c). Austenite grain boundaries are readily observable in the microstructures of the as-received sample as well as the HAZ samples. At the varied welding speed and power input, no noticeable modification of δ - phase throughout the microstructure was observed [6], only variations in grain size of austenite could be noticed. Also, inclusions and porosities in form of dark dots were noticed in some of the microstructures, none of micro-crackings were encountered during the investigation. Weld solidification cracking were present as white stretches in microstructures of the HAZ samples evaluated.

In addition, grain size of the phases could be seen to reduce with increasing welding speed [4]. Concerning effect of power inputs, it could be observed that the grains appeared to be coarser with increasing power input [6]. However, effect of power input on grain size appears to be relatively less than that of welding speed (Figs. 3a-c and 4a-c compared)



Figure 2: Micrograph of As – received Sample after Etching in Solution of 1 ml HCl + 3 ml HNO₃ + 1ml Glycerol at 400 xx.



Figure 3 (a-c): Micrographs of HAZ Samples at Slow, Moderate and Fast Speeds Respectively after Etching in Solution of 1 ml HCl + 3 ml HNO₃ + 1ml Glycerol at 400 xx.



Figure 4 (a-c): Micrographs of HAZ Samples at 4.60KW, 9.20KW and 12.00KW Power Inputs Respectively after Etching in Solution of 1 ml HCl + 3 ml HNO₃ + 1ml Glycerol at 400 xx.

Tensile Characteristic

Figs. 5 and 6 are the tensile stress-strain curves of the HAZ samples at the varied welding speed and power input, and as-received sample respectively. Plot of percent elongation against welding speeds and power inputs for the HAZ samples, and as-received sample are given by Figs.7 and 8. From the characteristics of the obtained graphs, Ultimate Tensile Strength (UTS) and Yield Strength (YS) of the HAZ samples at the varied welding speed were observed to increase in order of moderate(6.5 mm/s), fast (9.5 mm/s) and slow (2.5 mm/s) speeds [4]. Percent elongation (% E) was found to increase in reverse order of increasing UTS and YS [11] and when compared with the as-received sample, the tensile properties (UTS, YS and % Elongation) are relatively lower.



At varied power input, Ultimate Tensile Strength and Yield Strength of the HAZ samples were found to increase in order of 9.20KW, 4.60KW and 12.00KW (Fig. 6), and % Elongation in order of 12.00 KW, 9.20 KW and 4.6 KW (Fig.8), and when compared with the as-received sample, UTS and YS for the HAZ samples are lower.

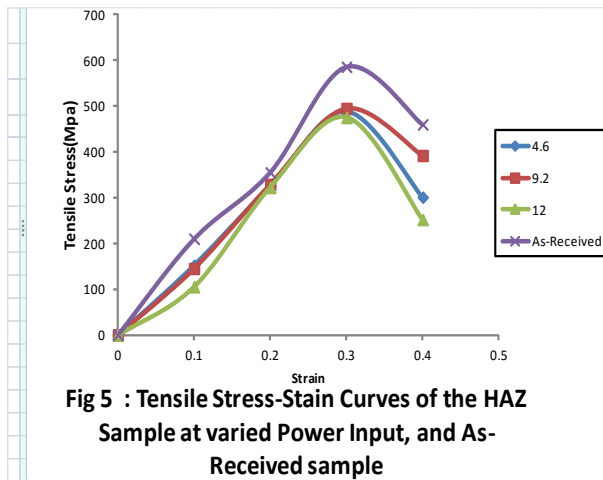


Fig 5 : Tensile Stress-Strain Curves of the HAZ Sample at varied Power Input, and As-Received sample

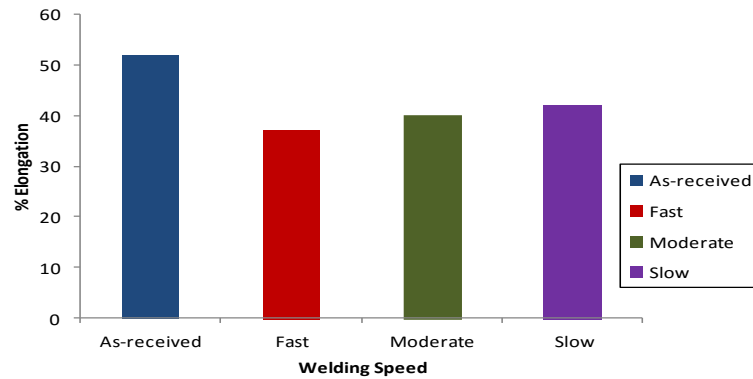


Fig. 7: Plot of Percent Elongation (%E) against a Range of Welding Speeds for HAZ Samples, and As-received Sample.

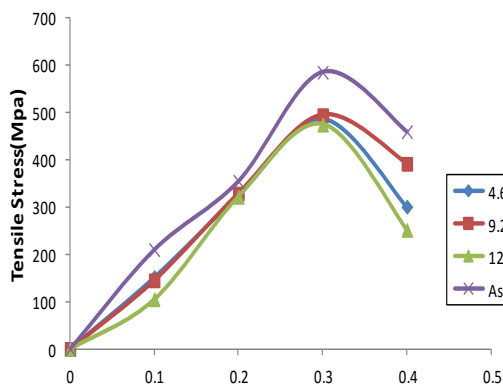


Fig 6: Tensile Stress-Strain curves of the HAZ Samples at a Range of Power Inputs, and As-received Sample

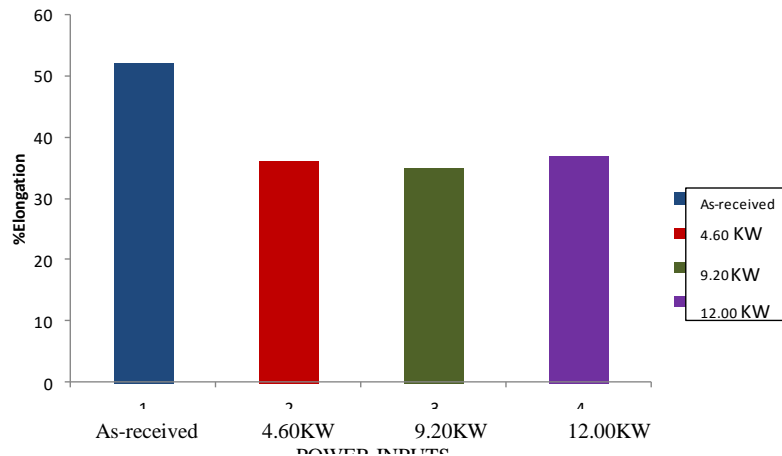


Fig. 8: Plot of Percent Elongation (%E) Against a Range of Power Inputs for HAZ Samples, and As-received



DISCUSSION

Microstructures

The obtained microstructural features of the as-received sample (Fig. 2) may have resulted from the initial treatments (pre-history) given to the sample prior welding [6,7], and the microstructural features of the HAZ samples at the varied welding speeds Figs.3 (a-c) and power inputs Figs. 4(a-c), may have been influenced by the chemical composition of the sample [6,11, and 12]. When Cr_{eq}/Ni_{eq} ratio is lower than 1.5, phase transition is trended to austenite, the existence of about 2 or 3 volume % ferrite in the weld metal reduces trend of crack susceptibility because more residual elements that spoil pureness can be easily solute in the ferrite [6], and the existence of a few percent of ferrite is useful to remove the tensile stress thereby preventing risk of micro cracking during solidification [6]. Based on schaeffer diagram, Cr_{eq}/Ni_{eq} ratio in this work was obtained as 1.9 as compared to the 1.5 proposed. Therefore more than 2 or 3 vol. % ferrite is expected to be present in the HAZ microstructures with attendant improved impact properties resulting from none micro-cracking during solidification [12]. Cracking in austenitic stainless steel is avoided as the proportion of primary ferrite in the mixed mode solidification increases [10, 12].

The present of ferrite phase in the microstructure of HAZ sample may have resulted from high temperatures of over $1000^{\circ}C$ attained in the regions of the HAZ during welding, the austenite fraction transforms to a high temperature ferrite [4]. Welding conditions may also have influenced the microstructural features of the HAZs samples. Welding conditions which result in higher heat input and/ or slow cooling tend to promote a greater reformation of austenite (beneficial); and an increase in the ferrite grain size, (non- beneficial) [6], fast cooling rates depress the reformation of austenite, resulting in higher level of retained ferrite which adversely affects ductility, toughness and corrosion resistance [10]. Transition in solidification from austenite to ferrite is related with cooling rather than composition of the austenitic stainless steel and austenite and ferrite microstructure occur [6].

The noticed variations in austenite and ferrite grains throughout the microstructures of the HAZ samples at the varied welding speed may have resulted from thermal cycling which produces differently featured heat- affected zone accompanied by microstructural changes in the engineered microstructure [13], it may also have resulted from a different cooling rates, at fast welding speed, heat input is low due to fast cooling rate, the weld freezes quickly with resulting small grains [5]. While, the relative coarse grains of the HAZ samples with increasing power input is attributable to slow cooling rate resulting from high heat input [10].

Effect of Welding Speed

A number of researchers have shown that welding parameters including speed have direct influence on the shape, depth of fusion, cosmetic appearance and heat input into the base metal [6, 12 and 14]. Hence, the improved UTS and YS characteristics of the HAZ samples in increasing order of moderate (5.5 mm/s), slow (2.5 mm/s) and fast (9.5 mm/s) welding speed and the poor ductility in decreasing order of improved Ultimate Tensile Strength and Yield Strength (Fig.5), and plot of % elongation against welding speed (Fig.7), are attributable to relative



penetration, depth of fusion and cracks resulting from influence of slow, moderate and fast welding speeds [6]. Faster speed reduces penetration and bead width, increase the likelihood of porosity and if taken to the extreme produces undercutting and irregular beads [7], and if too slow produces burn through [10], a combination of high arc voltage and slow welding speed can produce a mushroom shaped weld bead with solidification cracks at the bead sides [10], and decreasing the welding speed beyond a certain point may lead to decrease in penetration due to the pressure of the large amount of weld pool beneath electrode cushioning arc penetrating force [3], at fast speed, there is tendency for undercut, slag inclusion and porosity due to rapid cooling and as a result the weld freezes quicker [7], moderate welding speed allows for escape of gases from molten metal before solidification [14].

Also, changes in metallurgical structures (phase transformation) at a range of welding speed may have contributed to the observed tensile behaviour [7]. The weld thermal cycle produces differently featured HAZ accompanied by microstructural changes in the engineered microstructure [4], and transition in solidification from austenite to ferrite is related with cooling rate rather than composition of the austenite [10]. At fast welding speed, heat input is low and finer dendrite structures are produced due to increasing rates of solidification and cooling [11]. The observed superior tensile properties (UTS, YS and % elongation) of the as-received sample relative to the HAZ samples (Fig.5) may have resulted from balanced (optimum) microstructures [7]. Austenitic stainless steels are generally known to have higher tensile strengths and elongation, but lower yield strengths than ferritic stainless steels, and reduction in area is always the same [7].

Weld metal with a fully austenitic structure is more susceptible to cracking, finite amount of ferrite in the finished weldment is required to prevent the likelihood of hot cracking, and as a consequence, alloys 304 and 304L are designed to re-solidify with a small amount of ferrite to minimize cracking susceptibility [6]. Also, weld defects resulting from repeated thermal cycles may have contributed to the relative low tensile properties of the HAZ samples [4].

Effects of Power Input

The observed UTS and YS of HAZ samples at power inputs of 4.6 KW, 9.2 KW and 12.00 KW depicted by stress- strain curves (Fig. 6) and ductility characteristic shown in the plot of % elongation against a range of power inputs (Fig. 8), may be due to influence of heat input. Different zones in HAZ increased steadily with increasing power input [13], low heat input resulting from low power input, caused by low welding current at high welding speed can limit penetration and cause the weld bead to lift away from the surface being welded [12], if there is too much heat input, the weld bead grows in width and the likelihood of excessive penetration and spatter increase [4, 14]. Therefore, it at power input of 12.00 kW and above, excessive spatter and electrode overheating and cracking may have occurred; hence the observed decrease in UTS and YS characteristics is in order.

The observed superior ductility of the as-received sample as compared to HAZ samples may be explained by absent of cracks which are produced during cooling and solidification [13]. On the



other hand, the improved UTS and YS of the as received sample over the HAZ samples may be due to relative difference in volume fraction and grain size of austenite and ferrite phases [6].

CONCLUSIONS

The following conclusions were drawn from the results of this work:

- (i) Variations in volume fraction and grain size of austenite were observed in all the HAZ microstructures examined. In addition, chromium carbide formation and precipitation due to sensitization was observed at the grain boundaries.
- (ii) Ferrite phase was equally seen to be present in all the microstructures examined, also observed in the microstructures of HAZ sample were inclusions in form of dark spots which may have resulted from impurities such as moisture and dirt, and porosities in form of pin holes which may be due to effectiveness of shielding gases of, GMA welding process in protecting the work piece from atmospheric contaminants (nitrogen and oxygen).
- (iii) Optimum Ultimate Tensile Strength (UTS) and yield strength (YS) were obtained for HAZ sample at moderate (6.5 mm/s) welding speed, and optimum % elongation at slow welding speed. Optimum UTS and YS were obtained for HAZ sample at power input of 9.2 KW, and optimum % elongation at 12.00 KW.

REFERENCES

- [1] Korinko, P.S and Malene, S.H. Consideration for Weldability of Types 304L and 316L Stainless steels, *Journal of Science and Technology of Welding and Joining*. 32 (2). (2001) 301-421.
- [2] Cunat, P.J. (2007): The Welding Stainless Steels. Materials and Application Series, Vol. 3. Euro Inox Pp. 2-9, 23, 25-28. *An Electronic Manual* (www.euroinox.org/pdf/map/brochure_weldabilityEN.pdf15).
- [3] Gunaraj,. V, and Murugan. N Prediction of Heat-Affected Zone Characteristics in Shielded Metal Arc Welding of Structural Steel Pipes. *Welding Journal*, 4.(2) (2002) 94-105.
- [4] Bipin, K.S; and Tewarl, S.P. A Review on Effect of Arc Welding Parameters on Mechanical Behavior of Ferrous Metals/Alloys. *International Journal of Engineering Science and Technology*. 2(5); (2010) 1425-1432.
- [5] Woel-Shyan, L; Fan-Tzeng, and Chi-Feng, L. Mechanical Properties of 304L Stainless Steel SMAW Joints under Dynamic Impact Loading, *Journal of Materials Science* .40 (3) (2005).439-484
- [6] Ramazan Yilmaz and Huseyin Usun: Mechanical properties of Austenitic stainless steels Welded by GMAW and GTAW, *Journal of Marmara of Pure and Applied Sciences*. 18 (3) (2002) 97-113.
- [7] Eldridge, I.J. and Morrison, D.J.: Microstructures and Mechanical properties of Welded Fe-12 Cr-20 Mn Austenitic Stainless Steel, *Journal of Materials Engineering and Performance*. 3 (5) (1994) 606.
- [8] Ana Ma. Paniagua-Mercado; Victor M. Lopez-Hireta, Arture F. Mendez-Sanchez; Maribel L. Saucedo-Munoz: Effect of Active and Nonactive Fluxes on Mechanical



- Properties and Microstructure in Sub-merged-Arc Welds of A-36 Steel Plates. *Journal of Materials and Manufacturing processes*. 223 (4) (2007) 851-863.
- [9] Oyetunji, A., Kutelu, B. J., Akinola, A. O. Effects of Welding Speeds and Power Inputs on the Hardness Property of Type 304L Austenitic Stainless Steel Heat-Affected Zone (HAZ). *Journal of Metallurgical Engineering (ME)*. 2 (4) (2013). 124-129.
- [10] Fowless, R.J and Blake, S.E. Influence of Heat Input on Austenitic Stainless Steel Weld Properties. *African fusion*. 1 (2) (2008) 17-24
- [11] Akselen, O. M; Rorviki, G; Kvaale, P.E and VandDer Ejik, C. Microstructure Property Relationships in HAZ of New 13% Cr Martensitic Stainless Steels, *Welding Journal 160s*. An Electronic manual (www.files.aws/org/w/supplement/mortensen/aug99/) (2004)
- [12] El-Batany Abdel –Monem. Effect of Lazer Welding Parameters on Fusion Zone Shape and Solidification Structure of Austenitic Stainless Steels. *Elsevier Materials Letters*. 32 (2). (1997) 155-163.
- [13] Lothongkum, G; Chaumbai, P; Bhandhubanyong, P. TIG Pulse Welding of 304L Austenitic Stainless Steel in Flat, Vertical and Overhead Position. *Journal of Materials Processing Technology*: 32 (4) (1995) 410-414.
- [14] Juang S.C, and Tarng Y.S. Process Parameter Selection for Optimizing the Weld Pool Geometry in Tungsten Inert Gas Welding of Stainless Steel, *Journal of Materials Processing Technology*, 33(4) (2002) 44-48